Evaluation of Active Nucleation Mechanisms During Annealing of Commercial Purity Aluminium

L. Rabet*, I. Samajdar, B. Verlinden and P. Van Houtte

Katholieke Universiteit Leuven, Dept. MTM, de Croylaan 2, B-3001 Leuven, Belgium
* also at Royal Military Academy, Materials Lab., Renaissancelaan 30, B-1000 Brussels, Belgium.

ABSTRACT Developments of recrystallization textures were studied in cold rolled commercial purity aluminium by X-ray diffraction and by OIM (orientation imaging microscopy). During recrystallization, all the rolling texture components (except Goss {011}<100>) decreased, while Cube {001}<100> increased. Changes in recrystallization textures were due to frequency advantage or disadvantage of grains of different orientations, as relative grain sizes were mostly independent of microtexture. The frequency advantage for Cube was due to preferred nucleation of Cube grains from thin bands of Cube oriented material and such a scheme of preferred nucleation was dominated by stored energy differences.

Keywords: *Recrystallization, Texture, Cube, Commercial Purity Aluminium, Cold Rolling.*

1. BACKGROUND

Recrystallization texture in aluminium alloys remains a subject of considerable scientific and industrial interest [1-14]. Three possibilities for recrystallization texture exists in a typical thermo-mechanical processing: (I) the deformation texture is more or less reproduced after recrystallization, (II) randomization of texture takes place and (III) relatively insignificant components of the deformation texture become dominant after recrystallization [1,2]. Randomization of recrystallization texture may be caused by particle stimulated nucleation [1,3-5], while in (I) the relative role of preferred nucleation/growth is less pronounced. (III), on the other hand, remains a subject of intense scientific debate, as 'controversies' involving relative contributions from preferred nucleation and/or growth are still argued [1,2,4-11]. One way of avoiding such controversies is to describe the changes in recrystallization texture in terms of some physical parameters [1,5,11,16]. If a particular orientation g is 'strengthened' by recrystallization, then it has to be because of the fact that the g grains are more in number and/or larger in size. These can be captured very simply by the frequency and size advantage factors [6]. The frequency advantage can only be caused by preferred nucleation, either due to the stored energy criteria [2,9,10,11,13,14,16] and/or by micro-growth advantage or selection [2,5,7,8]. The size advantage, on the other hand, can be due to early preferential nucleation [2,11] and/or global growth advantage/disadvantage [2,7,9].

In this study, hot band structure of a commercial purity aluminium (AA1080) was cold rolled to 60 and 80% reductions. Developments in recrystallization textures were studied by bulk X-ray texture measurements and also by OIM (orientation imaging microscopy). Based on the experimental results, an effort will be made to evaluate the mechanism determining the formation of recrystallization textures in cold rolled commercial purity aluminium.

2. EXPERIMENTAL METHOD

DC cast commercial purity aluminium AA1080 (with Si = 0.04, Fe = 0.09 and Ti = 0.015 wt%) was hot rolled to a final thickness of 5 mm. Hot rolling involved breakdown (475 to 24 mm in thickness) and tandem (24 to 5 mm in thickness) rolling, with preheating at 553° (8 h) and an exit temperature of 328°C. The hot band microstructure consisted of bands of deformed (but well

recovered) material, which could not be recrystallized. The hot rolled material was subsequently cold rolled to 60 and 80% reductions. Cold rolled samples were annealed in a salt bath at 350°C and for different times, so as to obtain different amounts of recrystallization. Macrotexture measurements were obtained by the inversion of 4 incomplete X-ray pole figures using the software MTM-FHM [15]. The software uses a standard series expansion method. For volume fraction measurements X-ray orientation distribution functions (ODFs) were convoluted by suitable model functions using 16.5° Gaussian spread. Microtextural observations were made by OIM and sample preparation for aluminium is given in [4].

3. RESULTS

Fig. 1 shows the changes in textures through deformation and recrystallization and fig. 2 quantifies such changes in terms of the volume fractions of individual texture components of Goss {011}<100>, Brass {011}<211>, S {231}<346>, Cu {112}<111>, CG {012}<100>, H {001}<110>, CH {001}<210> and Cube {001}<100>. While Goss, Brass, S and Cu are typical deformation texture components [2,11], H are CH are potential PSN orientations [3,4]. As shown in the figures, after 60% reduction deformation texture components (with exception of Goss) strengthened, but did not change significantly from 60 to 80% reduction. After recrystallization Goss increased slightly, but the rest of the deformation texture components dropped significantly. A minor decrease in H was accompanied by a slight increase in CH.

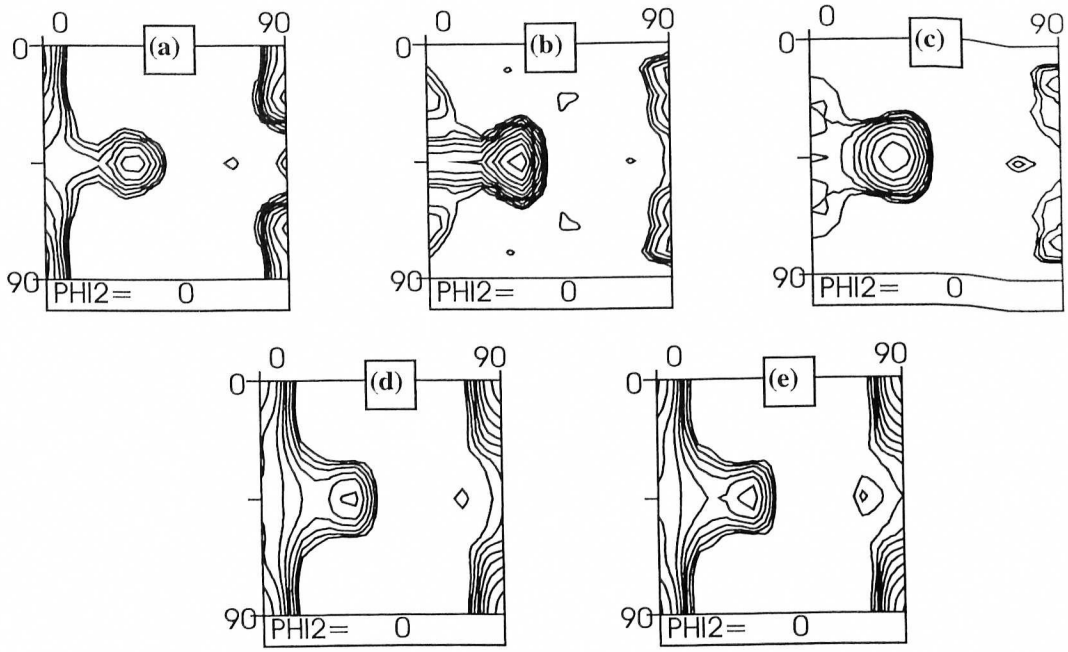

Fig. 1: $\varphi_2 = 0°$ sections of the X-ray ODFs for (a) hot rolled, (b) 60% deformed, (c) 80% deformed, (d) fully recrystallized 60% deformed and (e) fully recrystallized 80% deformed materials. Annealing times for full recrystallization were determined to avoid the possibility of post-recrystallization grain growth. Contour levels were drawn at 0.7, 1, 1.4, 2, 2.8, 4, 5.6, 8, 11 and 16 times random.

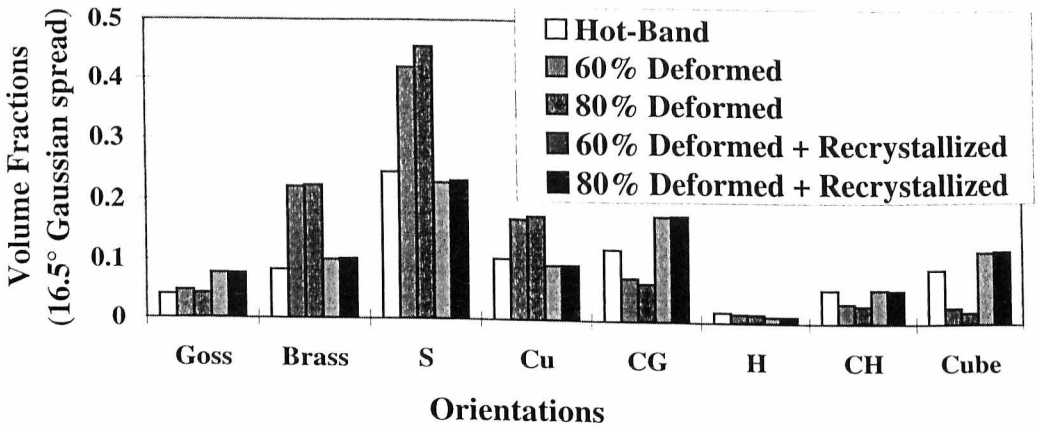

Fig. 2: Volume fractions of different texture components in different materials as in fig. 1.

The most important aspect of the recrystallization textures is the really significant increase in Cube and a slightly smaller increase in CG. The respective orientation change factors (OCFs, as in [16]) in Table 1 give a clearer quantification of the changes in textures through recrystallization. OCF for recrystallization is defined as $(V_R-V_D)/V_D$, where V_R and V_D are the respective volume fractions in the recrystallized and deformed samples [16].

Textural changes during recrystallization, as described in Table 1, clearly show a significant strengthening of the Cube component. As discussed earlier, such a strengthening may be due to a frequency and/or size advantage of the recrystallized Cube grains [2,6,11]. Fig. 3 shows the OIM micrograph of fully recrystallized 80% deformed material with Cube grains marked in different grey levels. Although a few large Cube grains are visible, Fig. 3 shows that in other regions also large non-cube grains exist. The maximum as well as the average grain sizes for Cube and non-Cube grains (grains misoriented by more than 20° from the ideal cube orientation) were roughly comparable in the recrystallized material after 60 respectively 80% deformation. The average Cube grain size measured using the OIM software was 25 (60% deformed) and 18 μm (80% deformed). Those values were quite similar for the non-Cube grains. In other words, there is no size advantage for Cube grains compared to grains with any other orientation and hence the changes in recrystallization textures were purely due to the frequency advantage or disadvantage for the respective orientations [2,6,11]. Evidently, such frequency advantage or disadvantage is caused by preferred nucleation. Fig. 4 is the OIM of 60% deformed material after a recovery anneal. As shown in the figure, deformed grains or bands of nearly one uniform orientation along the rolling direction (RD) typically characterize such a microstructure. Deformed Cube was only observed as thin bands of Cube oriented deformed material (see Fig. 4).

OCF	Goss	Brass	S	Cu	CG	H	CH	Cube
60%	0.61	-0.54	-0.45	-0.45	1.38	-0.26	0.67	3.28
80%	0.79	-0.54	-0.49	-0.46	1.74	-0.23	0.85	5.1

Table 1. OCFs (orientation change factors) of recrystallization after 60 and 80% reductions.

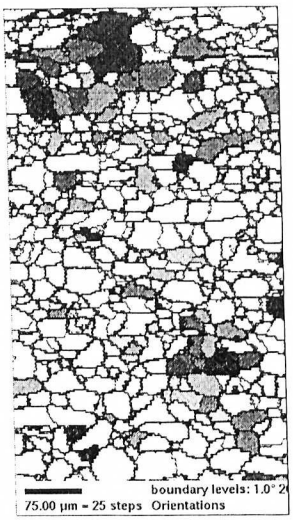

Fig. 3: OIM image of fully recrystallized 80% deformed material (350°C/4 minutes). Grain within 20° of the exact Cube are marked in grey levels (darker grains being closer to the exact Cube). Boundaries are drawn at 1-20° (light boundaries) and above 20° (dark boundaries) misorientations.

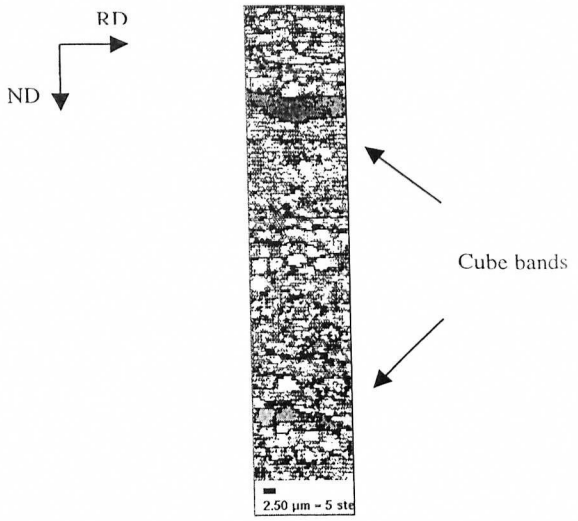

Fig. 4: As deformed (but recovered) OIM structure of 60% deformed material, showing Cube bands. Grain boundaries are drawn using the same conventions as in Fig. 3.

An effort was made to measure the spacings along the normal direction (ND) of such Cube bands and also the orientation of bands next to those Cube bands. Unlike warm deformed commercial purity aluminium [2,11], the patterns from cold rolled material were relatively weak (even after prolonged recovery). In addition, Cube bands often appeared 'broken' along RD, especially for the 80% deformed material. The spacings along ND of the Cube bands (broken or otherwise) were measured from scans of typically 40 µm width (along RD) but several hundred µm in length along ND, see Table 2. Note that most of these bands were rather broken and the spacings in Table 2 may not translate into exact volume fractions. As suggested in [2,11], volume or area fraction of the recrystallized Cube can be estimated by the simple geometrical relationship $N_C d_C/\lambda_C$, where d_C is the recrystallized Cube grain thickness along ND, λ_C the Cube bands spacing along ND and N_C the Cube nucleation factor [2,11] - i.e.the number of Cube grains per deformed Cube Band as measured or estimated along the ND. N_C values calculated from the measured area fraction, λ_C and d_C are listed in Table 2. Table 2 also contains the measured fraction of Cube bands next to S oriented deformed regions.

Deformation	Fraction of Cube Bands next to S	Cube band spacing λ_C (in µm)	N_C
60%	0.38	195	0.94
80%	0.48	120	0.83

Table 2. Features of Cube bands after 60 and 80% deformations.

4. DISCUSSION

The results clearly show that the changes in recrystallization textures are solely due to the frequency advantage/disadvantage of grains of different orientations, at least for the material of the present study. Note that the adjacent Cube grains (presumably coming from the same deformed Cube band) often shared low angle (1-5°) boundaries (especially along RD) and manual or even semi-automated measurements may indicate the presence of an actually non-existent size advantage in favour of such Cube grain clusters. There are two plausible mechanisms for the Cube frequency advantage: preferred nucleation due to the stored energy differences [2,10,11,14] and/or preferred nucleation due to micro-growth advantage or selection [2,7,8,11,14]. The micro-growth advantage in fcc Cube texture is usually considered [8,14] as the preferred nucleation from Cube bands with neighboring deformed S, as their 40°<111> boundaries are expected to be more mobile. Another possible explanation for such a preferred nucleation exists in the frame work of stored energy differences, as deformed Cube and S were observed to possess respectively the lowest and highest stored energies [10,11,13,14]. The present results, however, indicate that the Cube nucleation factor dropped at the higher reduction (this was possibly due to the lesser effective contributions from more broken/discontinuous Cube bands in the 80% deformed material). The increase of Cube bands next to deformed S in 80% deformed material doesn't result in a significantly higher Cube volume fraction after recrystallization, thus indicating that the role of micro-growth advantage (or the presence or absence of deformed S next to deformed Cube), though may be valid as a micro-mechanism for Cube recrystallization, may not be really significant in determining the strength of the final Cube recrystallization texture. Excluding the possibilities of a dominant role of micro-growth advantage/selection (which, according to the present measurements, is clearly the case), the final Cube recrystallization texture will be governed by: (a) presence of Cube oriented deformed regions and (b) preferred Cube nucleation from them.

Weiland and Hirsch [12] originally proposed that Cube grains/regions present prior to the deformation may form the deformed Cube bands. Indeed, in warm deformed aluminium original non-deformed Cube grains were observed to form the deformed Cube or the so called Cube bands [2,10,11]. As in warm plane strain-extruded/compressed commercial purity aluminium [2,11], each original Cube grain was observed to generate, on average, one deformed Cube band. In the present hot band structure, Cube regions existed as bands of deformed but recovered material, with an average spacing (as measured along ND) of 450 μm. If each such Cube region formed one deformed Cube band, then the expected Cube band spacings after 60 and 80% deformation will be 180 (450(1-0.6)) and 90 (450(1-0.8) μm respectively. The actual measurements (see Table 2) showed respective average spacings of 195 and 120 μm. This, in turn, indicates that about 0.92 and 0.67 of the hot band Cube regions could form the deformed Cube bands after 60 and 80% cold reductions. This should not be treated as an absolute index for Cube stability, as the results on macroscopic X-ray texture measurement (see Fig. 2) indicate a much stronger decay in Cube component. The differences between global and microtexture measurements possibly arrived from the facts that the deformed cube bands were often thinner than bands of other orientations (see Fig. 4) and they were hardly continuous but often broken or fragmented heavily along RD. This indicates that after the cold rolling reductions and the resultant heavy pancaking, only part of an original Cube region survived as semi-continuous stretch of deformed Cube region - the so-called deformed Cube bands. Another interesting issue was their proximity to the ideal Cube orientation. Only approximately 0.08 of the original hot band Cube was within 10° of exact Cube. This fraction increased to approximately 0.18 and 0.29 after respective reductions of 60 and 80%. In a word, although approximately 0.92 and 0.67 of the hot band Cube regions formed the basis of the deformed Cube bands after 60 and 80% reductions, for this remaining Cube the deviation from the exact Cube orientation decreased with increasing reduction. Another interesting feature of the deformed (but recovered) Cube bands was the high subgrain sizes and the relatively low misorientations among

neighboring subgrains (see Fig. 4) - both of which point to low stored energy [2,11,13,14,16]. In terms of subgrain misorientation/subgrain size or θ/d values [2,11,16], cold rolled S had the highest stored energy and Cube bands the lowest. This agrees with earlier observations in warm deformed aluminium [2,10,11]. It is clear that the stored energy differences between Cube and other orientations form the basis of preferred Cube nucleation [2,11].

5. CONCLUSIONS

1) The most important aspect of the cold rolled recrystallization textures was the significant strengthening of Cube orientation. This was solely caused by the frequency advantage of Cube grains, as Cube grains were comparable in size with grains of other orientations.

2) Preferred nucleation of Cube grains from thin Cube oriented deformed regions was responsible for the frequency advantage. Two issues were of critical importance: a) the presence of cube oriented deformed material or deformed Cube bands and b) their relative ability to form Cube grains.

3) Considering that deformed Cube bands originated from Cube oriented regions in the hot band microstructure, approximately 0.92 and 0.67 of such regions formed Cube bands after respective cold rolling reductions of 60 and 80%. However, for these Cube bands the deviation from the ideal Cube orientation decreased with increasing reduction.

4) The Cube nucleation factor dropped at 80% reduction, although presence of Cube bands next to deformed S (and hence possible effects of micro-growth advantage) actually increased. This might indicate a relatively insignificant role of micro-growth advantage/selection in determining the final Cube recrystallization texture. The low stored energies of the Cube deformed bands determined their ability to form recrystallized Cube grains.

ACKNOWLEDGEMENTS

Financial support of FKFO grant Nr G.0252.96 and the supply of the rolled material from Hoogovens Aluminium N.V. are well appreciated.

REFERENCES

[1] F.J. Humphreys and M. Hatherly, Recrystallization and Related Annealing Phenomena, Elsevier Sci. Ltd., UK, (1995).
[2] R.D. Doherty, I. Samajdar, C.T. Necker, H.E. Vatne and E. Nes, 16th Risf symp. on Mater Sci., eds. N. Hansen, D. Juul Jensen, Y.L. Liu and B. Ralph, Risf National Lab, Roskilde, Denmark, 1995, 1.
[3] L. Rabet, P. Ratchev, B. Verlinden and P. Van Houtte, ibid [2], 525.
[4] I. Samajdar, L. Rabet, B. Verlinden and P. Van Houtte, ISIJ Int., 38 (1998) 6, In Press.
[5] O. Engler, Mater. Sci. Tech., 12 (1996), 859.
[6] R.D. Doherty, Scripta Metall., 19 (1985) 8, 927.
[7] D. Juul Jensen, Acta Metall., 27 (1992), 533.
[8] B.J. Duggan, K. Lücke, G. Köhlhoff and C.S. Lee, Acta Metall., 41 (1993) 6, 1921.
[9] J. Hjelen, R. Ørsund and E. Nes, Acta Metall., 39 (1991), 1377.
[10] H.E. Vatne, R. Sahani, E. Nes, Acta Mater., 44 (1996), 4447.
[11] I. Samajdar and R.D. Doherty, Acta Mater., In Press.
[12] H. Weiland and J. Hirsch, Text. Microstruct., 18 (1991) 14, 647.
[13] A.A. Ridha, W.B. Hutchinson, Acta Metall., 30 (1982), 1929.
[14] I. Samajdar and R.D. Doherty, Scripta Metall., 32 (1995) 6, 845.
[15] P. Van Houtte, User Manual, MTM-FHM software, version 2, ed. by MTM-KULeuven, 1995.
[16] I. Samajdar, B. Verlinden, P. Van Houtte and D. Vanderschueren, MSE, A238 (1997), 343.